

Ultrasonic Imaging of Electrofusion Welded Polyethylene Pipes Employed in Utilities Industry

Arjun Prakash TK^{1,2}, Richard L O'Leary¹, and Anthony Gachagan¹

¹ Centre for Ultrasonic Engineering, University of Strathclyde

Glasgow, G1 1XW, UK

Phone: +44 (0) 141 548 4019

Fax: +44 (0)141 548 2950

E-mail: arjun.tk@eee.strath.ac.uk

Kevin Ross², Edward Clutton²

² Impact Solutions

Grangemouth, FK3 9XH, UK

Abstract

Electrofusion welding (EFW) is a widely used technique for joining polyethylene pipes in the oil, gas and water industry. Like many welding and joining methods, the joints created by EFW can exhibit a range of flaw types that can be attributed to process variables such as: poor preparation of the parent material, contamination of the weld surfaces prior to welding and operator and/or equipment failure during the welding process. This paper describes ultrasonic testing using 128-channel linear array with a DYNARAY system to acquire data from a range of joints created using EFW. The samples were created in the laboratory with a range of defects that represent those commonly observed in the field. The samples were subsequently destructively tested using tensile testing of the coupling-pipe interface. Good corroboration was achieved between the observed weld quality from the ultrasonic data and the weld strength determined by the destructive testing.

1 Introduction

High Density Poly Ethylene (HDPE) is used to transport a variety of materials such as potable water, waste water, chemicals, slurries, hazardous wastes, compressed gases etc⁽¹⁾. Some of the properties which make it an attractive option as a piping material are the low installation and maintenance costs, chemical inertness, flexibility, fatigue resistance and a smooth internal surface which gives excellent hydraulic efficiency⁽²⁾.

The most common methods of joining Polyethylene pipes are the butt fusion welding and electrofusion welding (EFW). The current discussion will be limited to the EFW technique where pipes are inserted into a polyethylene coupling which has an embedded wire for resistance heating (See Figure 1). A voltage is applied across the input terminals for duration equal to the Specified Fusion Time (SFT) and then allowed to cool. The duration may vary depending on coupling type and will be specified by the manufacturer. The procedure for EFW (based on the Water Industry Standards⁽³⁾, 2002) can be summarised as: pre-joint checks, preparation of the pipe surface, joint assembly and clamping, fusion cycle and visual joint checks on completion of the fusion cycle.

These steps involve inherent operator and/or equipment dependence which ultimately influence weld quality.

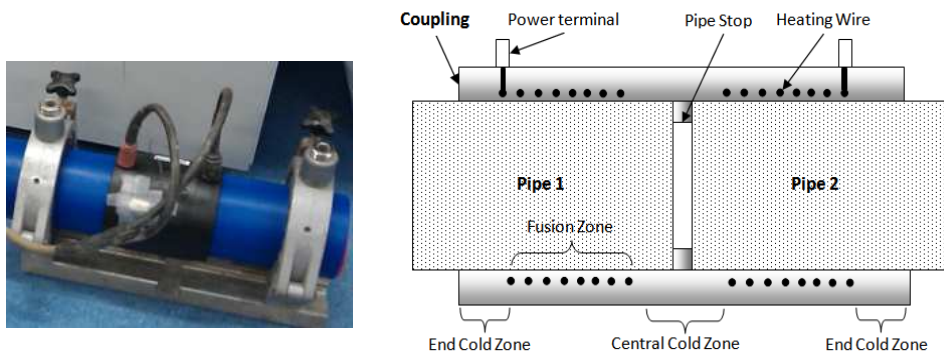


Figure 1: (Left) Pipe coupling assembly (Right) Cross-sectional schematic

Previously Shin et al ⁽⁴⁾ and Caravaca et al ⁽⁵⁾ have reported the use of B-Scans to detect defects in electrofusion welds. Shin et al ⁽⁴⁾ describes the use of this technique to detect an overheated joint based on wire dislocation, defect due to soil inclusion and an imperfect joint. Caravaca et al ⁽⁵⁾ describes an immersion inspection technique to detect defects due to lack of penetration, lack of fusion and reduced heating time which were corroborated with a crushing decohesion test.

This paper will describe the use of a 5MHz, 128 element array for the inspection of EFW samples. A range of welds were created to simulate defects due to:

- Surface contamination: Particulate surface contamination (with different particle types and sizes), and oliferous surface contamination,
- Errors in heating cycle (overheating, insufficient heating and two fusion cycles)
- Misalignment of pipes in the coupling.

The results from B-Scan inspection of the created samples are presented which demonstrates the capability of the technique to detect variability from a standard weld. The B-Scan data is then corroborated with the data obtained from a destructive testing of the inspected sample which gives both a quantitative and qualitative evaluation of the weld strength based on the observed peak *Load/Width* and the failure mode respectively. A probe carriage design with position encoding and adaptability to inspection scenarios involving different pipe dimension is also described.

2 Experiments and Results

2.1 Ultrasonic characterisation of PE80 and PE100

The velocity and attenuation in two grades of polyethylene commonly used in pipes – PE80 and PE100 were studied using the non-contact through transmission method ⁽⁶⁾. The transmitter and a receiver transducer were separated by a liquid coupling medium (water). The material to be characterised is placed between a transmitter receiver pair such that the sound waves travel through the specimen before reaching the receiver. ⁽⁶⁾ The correlation technique is used to find the value of time difference between the transmitted and reference waves which is substituted in the equation for longitudinal velocity. This method was carried out for a range of temperatures from 20 °C to 60 °C (See Figure 2).

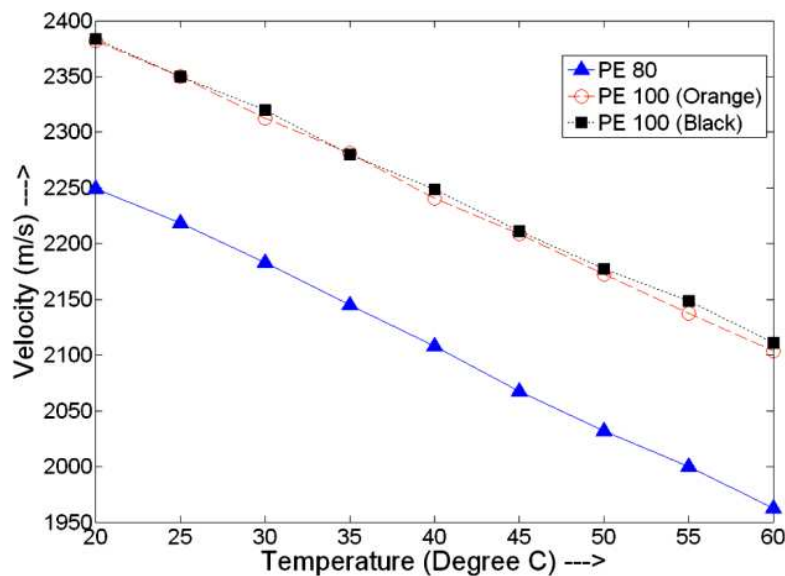


Figure 2: Plot of longitudinal velocity values for PE 80 and PE100 for different temperatures

The values obtained from the non-contact method showed good correlation with the values obtained from the contact through transmission method (where transducers were placed in contact with the sample). The non-contact method was also used to determine transverse velocity and attenuation characteristics of PE80 and PE100 for different temperatures.

2.2 Preparation of sample defects

A range of electrofusion weld samples for pipe diameter 110 mm and 125 mm were created to simulate common defects that could occur in the field. These include:

- (a) Defects due to incorrect heating cycle - Overheated and insufficiently heated samples were created by varying the time for which voltage is applied across the coupler terminals. An invalid double weld was also created by carrying out the

welding process once for the SFT and then carrying out another weld for half the SFT once cold.

- (b) Surface contamination - The contaminant was introduced on the pipe surface before inserting into the coupling and starting the welding process. The different contaminants that were used include water, silicone grease, grease from food, kaolin (<106 um), talc (<40um, <75um, <106um), sand (< 290um), silica gel (<1mm) and soil (varying particle sizes).
- (c) Misalignment - Pipes were not properly aligned in the coupling before welding, resulting in tapering and lack of fusion in areas further away from the coupling.

2.3 Transducer selection and ultrasonic inspection setup

For the 110 mm coupling, the embedded heating wire has a diameter of 0.6 mm with a pitch 2 mm. An inspection wavelength that is less than the wire diameter would be expected to resolve the wires and any defects that appear between them. The velocity obtained in the ultrasonic characterisation experiment presented in Section 2.2 was used to calculate the inspection wavelengths for different frequencies. A 5MHz probe which would result in a wavelength of approximately 0.4 mm in the sample at room temperature was considered a good trade-off between resolution and wave attenuation. The final inspection setup involved a 5MHz linear array with 128 elements, Zetec *Dynaray* Phased array controller (Shown in Figure 3) and a PC running the Zetec *Ultravision* software.



Figure 3: (Left) Zetec *Dynaray* phased array controller and (Right) Vermon 5MHz, 128 element probe

A linear B-Scan (electronic scanning) is carried out, where a subset of elements are excited, the relative phase of the excitation focusing energy to a particular depth in the sample being interrogated. The focal law is then multiplexed along the complete probe length (aperture) to cover all the elements ⁽⁷⁾.

A carriage has also been designed for manipulating the probe around the cylindrical inspection surface (See Figure 4). A pulley and cable based approach was selected to facilitate adaptability across different pipe diameters by changing the cable length. The design also incorporates a quadrature encoder to determine the relative position on the coupling surface.

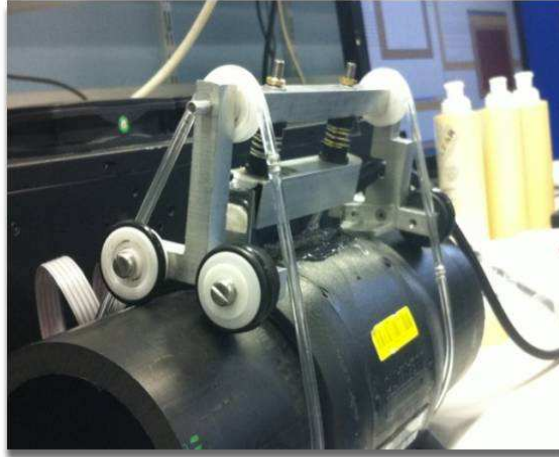


Figure 4: Carriage for manipulating the array along the inspection surface

In the results presented, a contact inspection methodology was used; with gel facilitating the energy coupling into the sample. The disadvantage of this method is the inaccessibility of some areas such as the manufacturer labelling and the tapered ends. However, from the results obtained, it was observed that despite the reduced inspection area, sufficient data was available for defect detection.

2.4 Analysis of B-Scan data

Figure 5 shows the B-Scan image of a standard weld next to an actual cross-section. The standard weld was produced by adhering to the SFT prescribed by the coupling manufacturer and following the practices prescribed by Water Industry Standards ⁽³⁾.

In the B-Scan image, the wires and the central cold zone are visible as strong reflections. Pipe inner wall can be observed below the heating wires. The Eigen Line ⁽⁸⁾ also referred to as the Heat Affected Zone ⁽⁵⁾ appears as a weak reflection above the wires and indicates the extent of heat input to the weld. This is the boundary of the region around the heating wires where polyethylene exists in the molten state during the welding process. Reason for the existence of the Eigen line has been attributed to the formation of voids at the solid-liquid interface ⁽⁸⁾. Shi et al ⁽⁸⁾ have shown that the distance between heating wires and Eigen line follow an approximately linear relationship with the welding time. If this distance is known for a correct heating cycle, variance in the heat input into the system can be determined based on the Eigen line position observed in the weld being inspected.

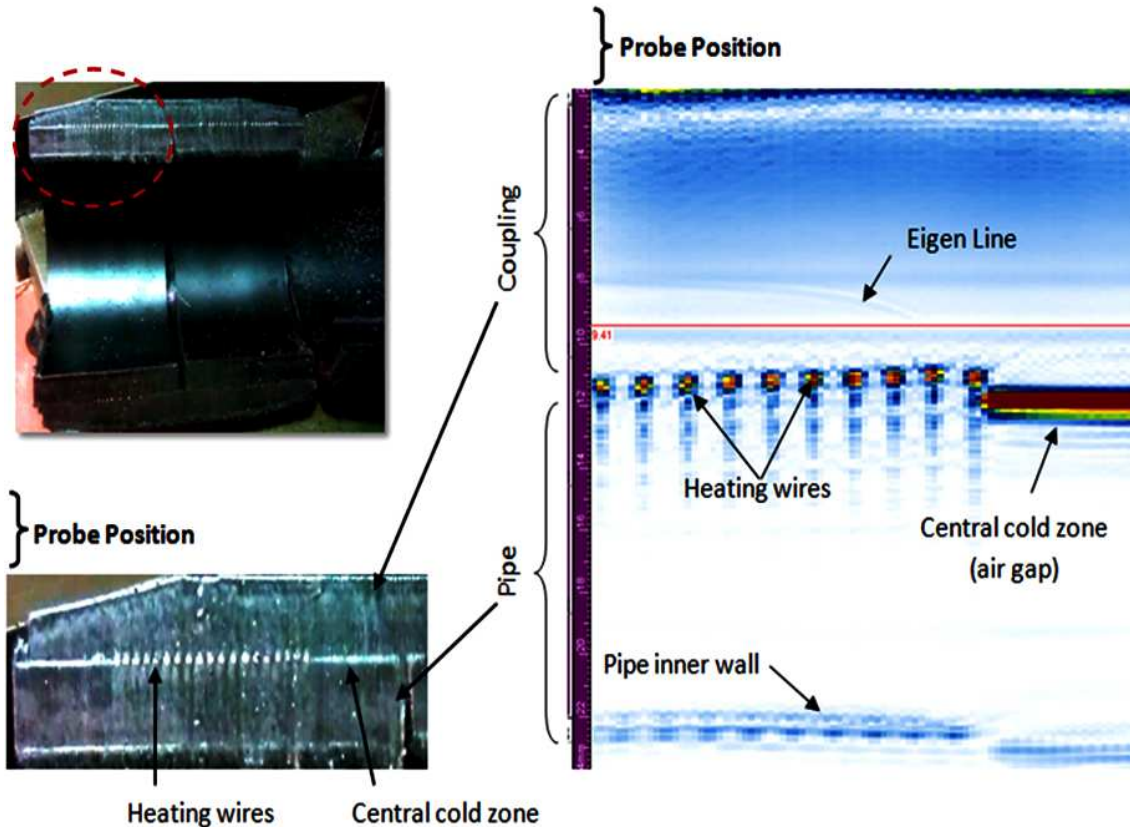


Figure 5 (Right) B-Scan of a standard weld (Top Left) Cross-section of an electrofusion weld (Bottom left) Region of the cross-section visible in the B-Scan

Figure 6 to Figure 11 shows sections of B-Scans acquired from the sample defects, which can be compared to the standard weld result shown in Figure 5. In the sample which was welded twice (Figure 6) two Eigen lines are visible. In the B-Scan of the weld for which the fusion time was restricted to 0.6 times the SFT (Figure 7), the Eigen line is much closer to the heating wires. For the weld for which the fusion time was twice the SFT (Figure 8), the Eigen line is further away from the heating wire, and in addition the heating wires are displaced from their original position and reflections are observed from between the wires due to material degradation. In Figure 9, for the misaligned weld, strong reflections from beneath the wires indicate a lack of fusion. Similarly, lack of fusion caused due to oliferous contaminant (Silicone grease) and particulate surface contaminant (Talc with particle size <40 um) can also be seen as reflections from beneath the heating wires in Figure 10 and Figure 11 respectively. For contaminants with particle size much lesser than the inspection wavelength such as the one shown in Figure 11, reflections from beneath the wires were picked up mainly in areas of particle aggregation and were found to be challenging.

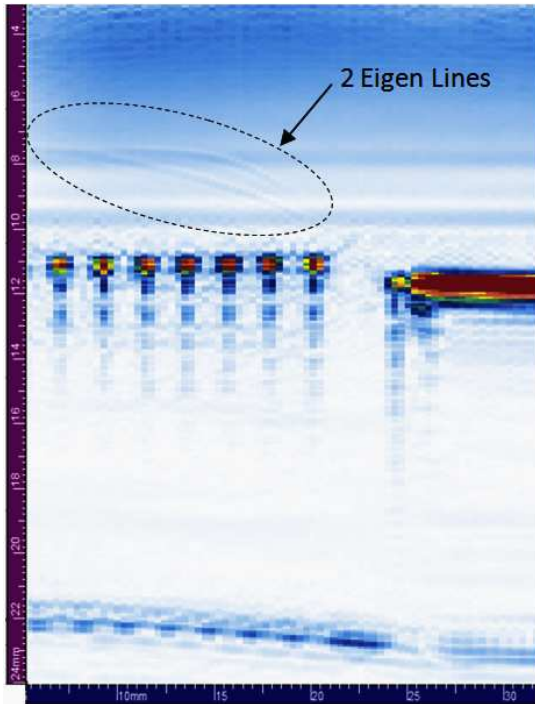


Figure 6: Fusion cycle carried out twice

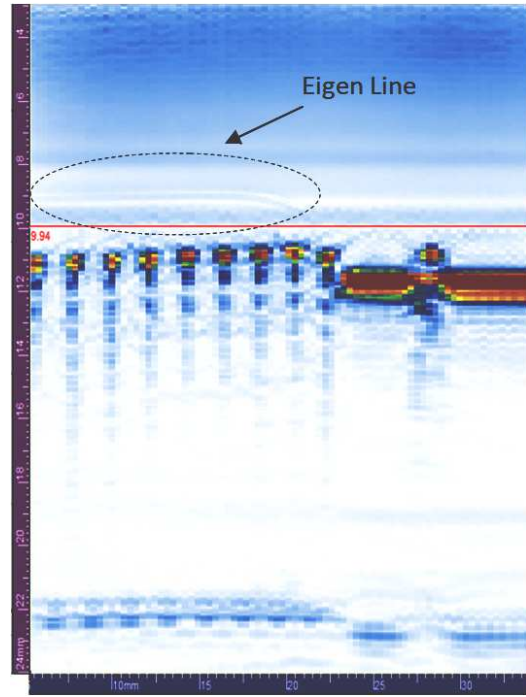


Figure 7: Insufficiently heated (fusion time = $0.6 \cdot SFT$)

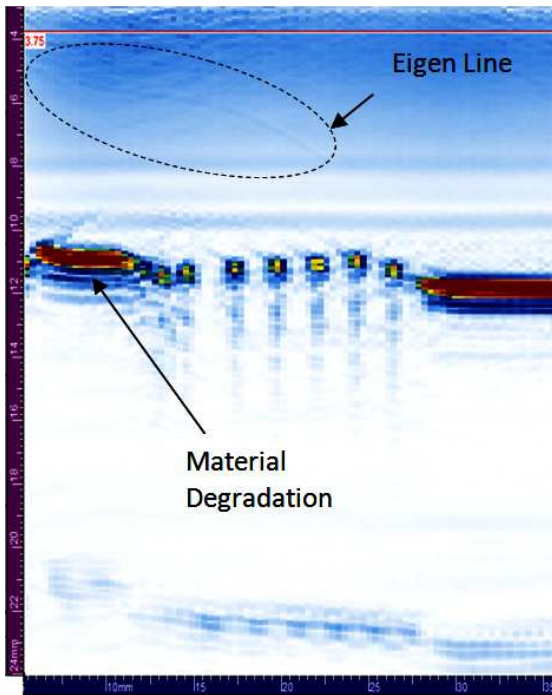


Figure 8: Overheated (fusion time = $2 \cdot SFT$)

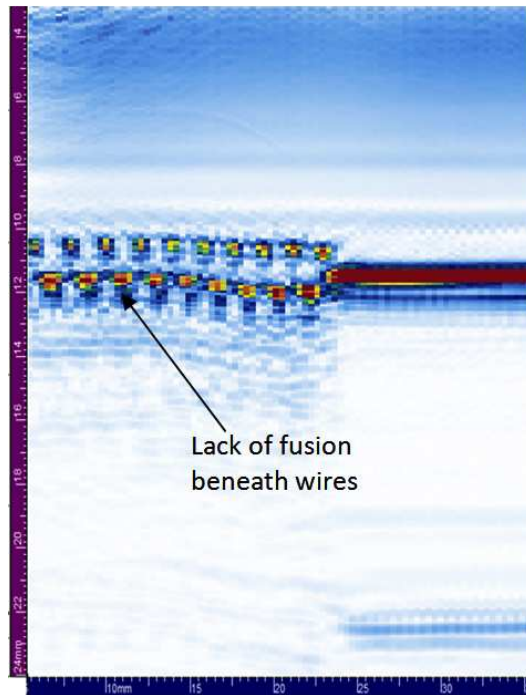


Figure 9: Weld carried out with pipes misaligned

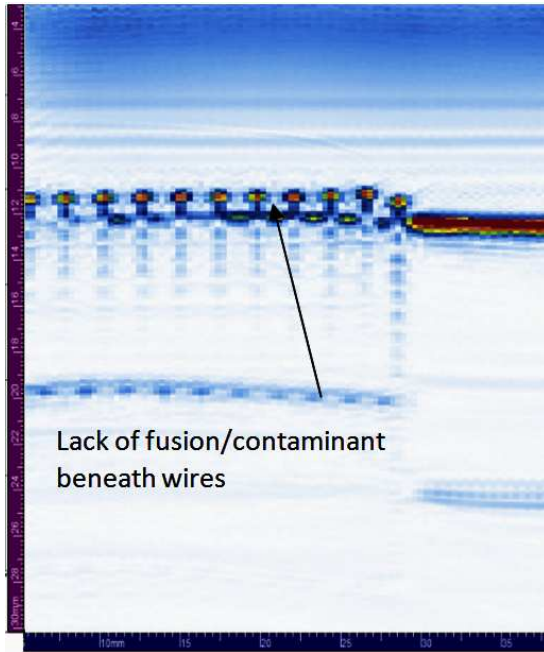


Figure 10: Oily surface contaminant (Silicone Grease)

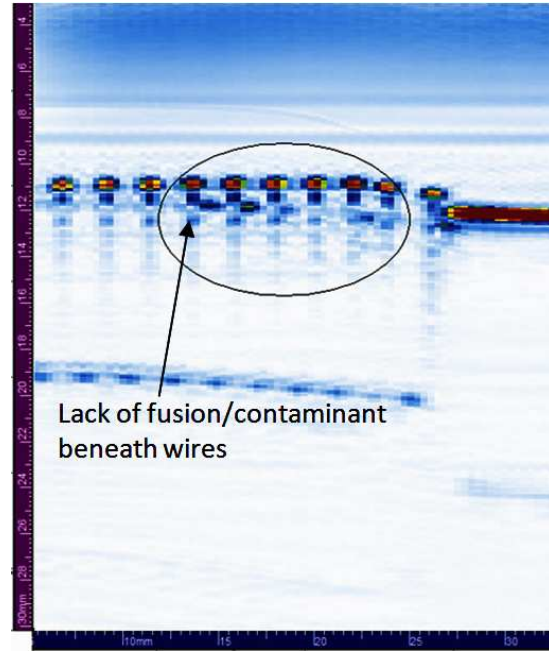


Figure 11: Particulate surface contaminant - Talc (<40um)

2.5 Destructive testing and corroboration with Ultrasonic inspection results

Once the samples were ultrasonically inspected, they were destructively tested by the double cantilever cleavage test. Six rectangular sections of diameter approximately 20 mm were cut from each weld using a band saw, ensuring the pipe and coupling surfaces remained parallel to the axis formed by the weld interface. Two holes were drilled at the cold zone end – one through the coupling and the other through the pipe, to fit metal pins. The *Instron* tensile testing machine was used to pull the joint apart at a constant rate (See Figure 12), with data being logged for the *Force/Displacement* value. From this data, the mean value for a weld is noted and used to determine weld strength.



Figure 12: (Left) Instron tensile testing device (Right) Weld being pulled apart during destructive testing

Figure 13 shows the mean load/width value obtained for the samples described in section 2.4 and the error bars indicate the standard deviation. It can be seen that the weld fused at $0.6 \times \text{SFT}$ does not show a significant overall reduction in strength despite a large standard deviation. This could be attributed to the tolerance levels associated with the amount of heat required for maximum weld strength. All other samples show a significant reduction in strength.

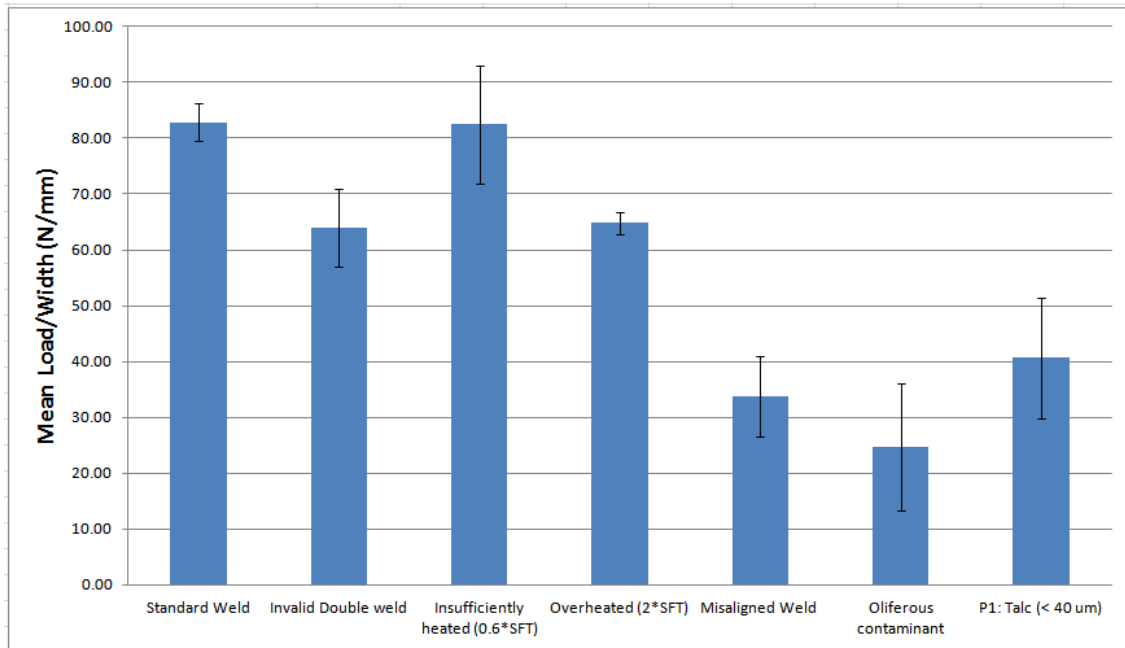


Figure 13: Mean values of *Load/Width* obtained for different welds during the destructive testing

A qualitative assessment of the weld strength can be carried out from the type of failure observed during the tensile test (See Figure 14). For a good weld, failure involved significant drawing of the material between the wires and is referred to as a ductile failure and was observed in the standard weld. Brittle failure (or a mix of both brittle and tensile failure) was observed in poor welds characterised by very little drawing of the material and failure occurs at a much lower load.

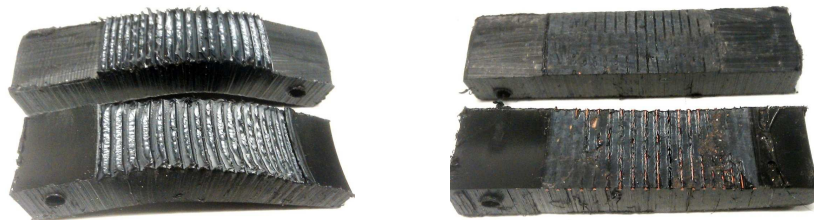


Figure 14: Example of (Left) ductile failure in the standard weld sample and (Right) brittle failure in the sample with surface contamination (soil)

3 Conclusions

Using the B-Scan imaging technique, it was possible to detect the majority of defects which can be introduced into electrofusion welds. Detection of particulate contaminants can be challenging in some scenarios where the size of the inclusion is much lesser than the inspection wavelength. In addition to the 110 and 125 mm pipe samples, this technique was also successfully applied to two real-world welds (75 mm and 180 mm diameter) which had failed in the field; and is expected to be scalable to other pipe dimensions.

Acknowledgements

Knowledge Transfer Partnership (KTP) and the West of Scotland KTP centre for supporting this project with Impact Solutions, Grangemouth.

References

1. 'High-Density Polyethylene Pipe Systems: Meeting the challenges of the 21st Century', Plastics Pipe Institute, www.plasticpipe.org, [online], Available: http://www.plasticpipe.org/pdf/high_density_polyethylene_pipe_systems.pdf
2. 'Second Edition Handbook of PE Pipe', Plastics Pipe Institute, Chapter 1-Introduction, [online], Available: http://plasticpipe.org/publications/pe_handbook.html
3. 'Specification for the Fusion Jointing of Polyethylene Pressure Pipeline Systems Using PE80 and PE100 materials', WIS 4-32-08, Issue 3, April 2002.
4. H. J. Shin, Y. H. Jang, J. R. Kwan, and E. J. Lee, 'Nondestructive Testing of Fusion Joints of Polyethylene Piping by Real Time Ultrasonic Imaging', NDT.net, Vol 10, No 3, March 2005, ISSN: 1435-4934.
5. D S Caravaca, C Bird, and D Kleiner, 'Ultrasonic phased array inspection of electrofusion joints in polyethylene pipes', Insight Vol 49, No 2, pp 83-86, February 2009.
6. O'Leary, R.L., 'An Investigation into the Passive Materials Utilised within the Construction of Piezoelectric Composite Transducers', Ph.D. Thesis, University of Strathclyde, Glasgow, Scotland, UK (2003).
7. 'Introduction to phased array ultrasonic technology applications', R/D Tech guideline, Olympus NDT, ISBN 0-9735933-0-X.
8. J.S.J Zheng, W. Guo, P. Xu, Y. Quin, Shangzhi Zuo, 'A model for predicting Temperature of Electrofusion Joints of Polyethylene Pipes', Journal of Pressure Vessel Technology, pp 061403-1 – 061403-8, Vol 131, December 2009.